

A COMPARISON OF DIFFERENT METHODS FOR DETERMINATION OF ELASTIC-PLASTIC R-CURVES

H.-J. Kaiser and K. E. Hagedorn

**Max-Planck-Institut für Eisenforschung, Max-Planck-Straße 1,
4000 Düsseldorf, Federal Republic of Germany**

ABSTRACT

R-curves of CT-specimens with a width of 100 mm and of different thicknesses were obtained for a high strength steel. Different methods were applied to characterize the crack growth resistance for elastic-plastic material behaviour. It is described either in terms of COD, J-integral and formal K-values calculated from these elastic-plastic parameters or in terms of effective K-values according to the ASTM-recommendation E 561. A comparison of R-curves determined by these different methods was made. The crack length was measured by the potential drop technique. The R-curves using the potential drop technique are compared with R-curves determined by the multiple specimen technique. The influence of temperature and specimen thickness on the R-curves is discussed.

KEYWORDS

Crack propagation; fracture properties; R-curves; elastic-plastic fracture mechanics; crack length measurement.

INTRODUCTION

The R-curve concept has been developed to describe material toughness development from slow-stable crack initiation up to specimen failure (Srawley and Brown, 1965). For materials with steeply rising R-curves, a more realistic estimation can be made of the true load carrying capability of flawed structures as it can be done using conservative criteria referring to the onset of crack growth.

The R-curve is determined simply by a plot of crack growth resistance versus crack growth. For linear-elastic material behaviour the crack growth resistance can be described by the linear-elastic stress intensity factor K. However, steels are generally used at temperatures near the upper shelf temperature range, where there is extensive plasticity, then concepts other than the linear-elastic K-concept have to be applied for describing the rise of crack growth resistance with

increasing crack growth. The crack growth resistance can be expressed in terms of elastic-plastic parameters in different ways. By using yielding fracture mechanics concepts, in particular the COD and J-integral concept, formal K-values can also be derived for elastic-plastic material behaviour. Furthermore, elastic-plastic R-curves can be evaluated using the ASTM-recommendation E 561. According to this recommendation effective K-values for ductile materials can be derived from effective crack lengths which are calculated from the load-displacement curve and a calibration curve for the specimen compliance.

EXPERIMENTAL DETAILS

The fracture mechanics experiments were carried out on an electro-slag remelted high strength steel 30CrNiMo8 having a room temperature yield strength of 850 N/mm². The tests were conducted on compact tension (CT) specimens of width 100 mm and thicknesses ranging from 5 to 20 mm.

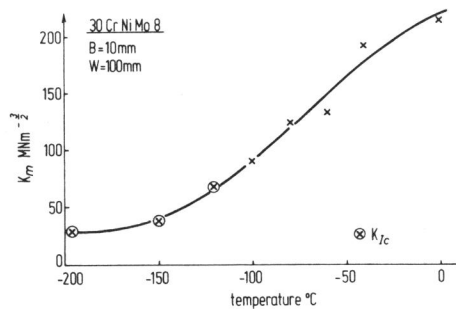


Fig. 1 Temperature dependence of fracture toughness K_m calculated from maximum load for 100 mm wide and 10 mm thick CT-specimens of the steel 30 CrNiMo 8.

The transition temperature curve of the steel 30 CrNiMo 8 obtained by the fracture mechanics experiments is shown in Fig. 1. Experiments with specimens of different thicknesses were carried out at 0°C near the upper shelf region of the rather shallow transition curve. The three points near the lower shelf were obtained from a steel 30CrNiMo8 of a different charge, this might give rise to a little more scattering in the lower shelf region. In the whole of the shallow transition region a "pop-in" behaviour was found and only specimens tested at 0°C showed no "pop-in" before reaching maximum load.

The displacement was measured by a double clip-gauge at two locations in the load line and on the specimen surface. To monitor the stable crack growth a DC potential drop equipment was used. The potential drop at the crack tip was measured and for temperature-compensation divided by a reference potential measured on the specimen surface beside the crack (Hagedorn and Rüdiger, 1977). The amplified, filtered and divided output signal of the potential drop device U_{out} was recorded together with the load line displacement (see Fig. 2). A dis-

tinct increase in the slope of the U_{out} -load line displacement record was taken as the point for crack growth initiation. This point is indicated in Fig. 2 by an arrow.

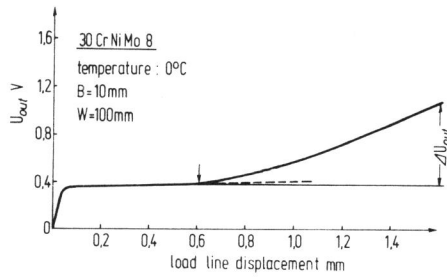


Fig. 2 Record of the potential drop device output signal U_{out} versus load line displacement for a 100 mm wide and 10 mm thick CT-specimen of the steel 30CrNiMo8.

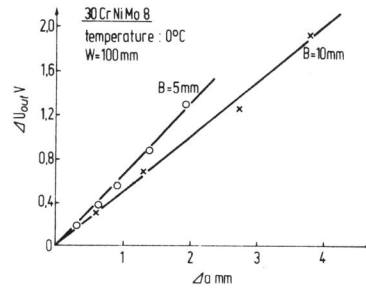


Fig. 3 Calibration curves of the potential drop device ΔU_{out} versus crack extension Δa for 100 mm wide CT-specimens of the steel 30CrNiMo8.

Fig. 3 shows calibration curves for the potential drop device for the 5 mm and 10 mm thick specimens. The curves were obtained by loading four or five specimens up to different displacement levels (see Fig. 7). The specimens were then unloaded and the fracture surfaces were marked by a heat-tinting treatment. Finally, the specimens were fractured in liquid nitrogen. ΔU_{out} represents the difference in the output signal from the initiation of stable crack growth to the end of loading. The crack growth Δa was evaluated by measuring the crack extension at nine points along the crack front and averaged to give mean values. A good linear approximation can be made for the calibration points of both specimen geometries, but there is a slight difference in the slopes of the calibration curves for the two different geometries.

To characterize the crack growth resistance for elastic-plastic material behaviour, yielding fracture mechanics concepts were applied. COD- or δ -values were extrapolated from the load line displacement measurements. The extrapolation technique according to the British standard BS 5762-1979 was used for calculating the crack opening displacement δ of the CT-specimens neglecting the fact, that only SENB-specimens are admitted in this standard.

$$\delta = \frac{K^2 (1-\nu^2)}{2 \cdot R_{p0,2} \cdot E} + \frac{V_p 0,4 (W-a)}{(0,4W+0,6a+z)} \quad (1)$$

$R_{p0,2}$ = yield strength; E = Young's modulus; ν = Poisson's ratio; V_p = plastic component of clip-gauge displacement; W = specimen width; a = crack length; and z = distance from clip-gauge position to load line.

Formal K-values can be calculated from the δ -values using linear-elastic fracture mechanics relations:

$$K_{\delta} = \sqrt{\beta \cdot R_{p0,2} \cdot \delta \cdot E / (1-\nu^2)} \quad (2)$$

For the stress state dependent factor β a constant value of $\beta = 2$ was assumed.

For the J-integral evaluation a formula developed by Merkle and Corten (Clarke and co-workers, 1978) was used:

$$J = \frac{2A}{B(W-a)} \frac{1+\alpha}{1+\alpha^2} \quad (3)$$

A = area under the load-displacement diagram; B = specimen thickness; and

$$\alpha = \sqrt{\left(\frac{2a_0}{W-a}\right)^2 + 2 \left(\frac{2a_0}{W-a}\right) + 2} - \left(\frac{2a_0}{W-a} + 1\right) \quad (4)$$

Formal K-values can also be derived from the J-values using linear-elastic fracture mechanics relations:

$$K_J = \sqrt{E \cdot J / (1-\nu^2)} \quad (5)$$

Another way of obtaining an elastic-plastic R-curve is given in the ASTM-recommendation E 561. According to this recommendation the R-curve can be expressed in terms of effective K-values versus crack extension or effective crack extension. For ductile materials the effective crack length and the effective K-value should be calculated from the load-displacement diagram and a calibration curve for the elastic specimen compliance.

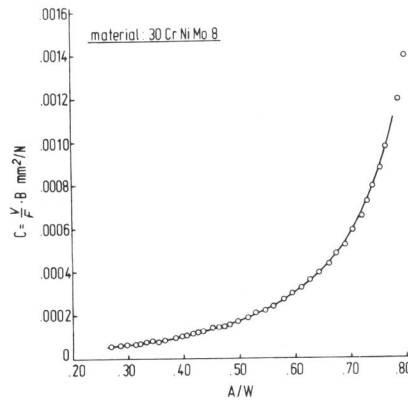


Fig. 4 Calibration curve for the specimen compliance C versus crack length ratio a/W for the steel 30CrNiMo8.

The experimentally-determined compliance calibration curve is shown in Fig. 4. This curve was obtained by fatigue loading of a CT-specimen.

The experimental points are smoothed with cubic spline functions.

RESULTS

In Figures 5 and 6 R-curves of CT-specimens of different thicknesses are shown in terms of δ - Δa and J - Δa . Δa is the average physical crack growth calculated from the potential drop measurement. Both methods produce a similar picture of the rise of crack growth resistance with stable crack extension. The initiation point of the R-curves is not the same for all thicknesses; it seems that for thinner specimens the stable crack growth begins at lower δ - and J -values. The R-curve of the 5 mm thick specimen rises with the steepest slope because of the extensive plastic deformation. With increasing specimen thickness the slopes of the R-curves are distinctly decreased.

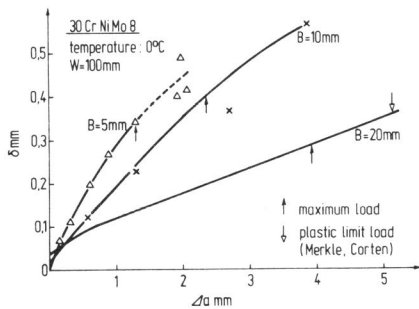


Fig. 5 Effect of thickness on R-curve behaviour δ - Δa for 100 mm wide CT-specimens of the steel 30CrNiMo8.

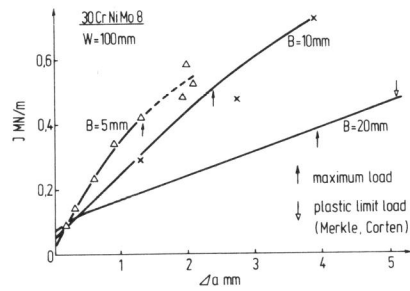


Fig. 6 Effect of thickness on R-curve behaviour J - Δa for 100 mm wide CT-specimens of the steel 30CrNiMo8.

To check the crack length calculation obtained by the potential drop measurement several specimens of 5 and 10 mm thickness were loaded up to different displacement levels, unloaded and the crack growth marked by a heat-tinting treatment. The fracture surfaces of four 10 mm thick specimens, which were loaded to different displacement values, are illustrated together with the load-displacement diagram in Fig. 7. The arrows indicate the points to which the specimens were loaded. As in the R-curves (Fig. 5, Fig. 6), the stable crack growth begins well before maximum load, soon after the load-displacement curves deviate from the linear part. The points of the R-curves obtained by the multiple specimen technique are marked in Fig. 5, 6 and 8. The points are well matched to the R-curves based on the crack extension measurement with the potential drop device.

To estimate the extent of plastic deformation of CT-specimens, several formulas have been developed by different authors for calculating the plastic limit load where fracture occurs under fully plastic conditions. Merkle and Corten (1974) have derived the following expression for the plastic limit load of CT-specimens:

$$F_{GY} = 1,26 \cdot R_{p0,2} \cdot B \cdot (W-a) \cdot \gamma \quad (6)$$

$$\gamma = (\sqrt{2} \sqrt{1+(a/W)^2} - (1+a/W)) / (1-a/W)$$

It has been found that limit load values calculated by this procedure do in fact provide a very close lower bound to existing experimental limit load data of CT-specimens (Merkle and Corten, 1974). For the tested specimens formula (6) agrees better than 10 % with the expression derived from numerical calculations by Schmitt and Keim (1979). In Figures 5, 6 and 8 arrows indicate the attainment of plastic limit load according to formula (6). For the 5 and 10 mm thick specimens the fully plastic condition was not exceeded until the end of loading, though it was almost reached. Only for the 20 mm thick specimen was the plastic limit load exceeded after considerable crack extension and after the attainment of maximum load.

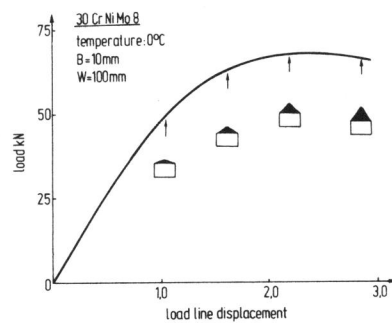


Fig. 7 Load-displacement record and fracture surfaces of 100 mm wide and 10 mm thick CT-specimens loaded up to different displacement levels for the steel 30CrNiMo8.

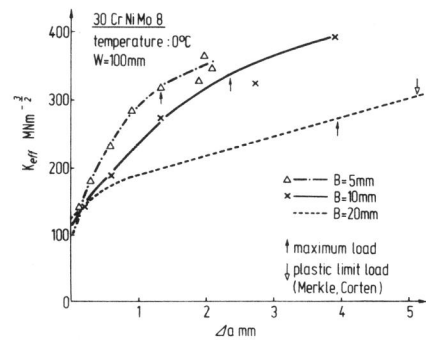


Fig. 8 Effect of thickness on R-curve behaviour $K_{eff}-\Delta a$ for 100 mm wide CT-specimens of the steel 30CrNiMo8.

In Figure 8 R-curves of the three CT-specimens of different thickness are shown in terms of $K_{eff}-\Delta a$. The picture is similar to those diagrams where $\delta-\Delta a$ and $J-\Delta a$ are plotted, discussed above.

A comparison of the elastic-plastic R-curves obtained in terms of K_{eff} , K_J and $K_\delta-\Delta a$ is made for the 10 mm thick specimen in Fig. 9. An R-curve in terms of the linear-elastic K as a function of Δa is also shown. This curve lies well under the elastic-plastic R-curves and already differs at small crack extensions. However, the elastic-plastic R-curves in terms of $K_{eff}-\Delta a$ and $K_J-\Delta a$ agree well up to and beyond the attainment of maximum load whereas the R-curve in terms of $K_\delta-\Delta a$ rises steeper. A similar behaviour was observed for the other tested specimens of different thickness. Noticeable differences between the elastic-plastic R-curves in terms of $K_{eff}-\Delta a$ and $K_J-\Delta a$ first occurred at very high crack extensions where the maximum load was already exceeded.

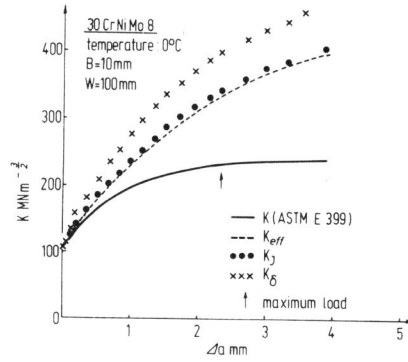


Fig. 9 Comparison of R-curves using linear-elastic and elastic-plastic methods for 100 mm wide and 10 mm thick CT-specimens of the steel 30CrNiMo8.

Figure 10 shows the influence of temperature on the elastic-plastic R-curves plotted in terms of $K_{eff}-\Delta a$. The R-curves were obtained at -100°C (in the lower transition region), at -40°C (in the upper transition region), and at 0°C (near the upper shelf of the transition temperature curve), see Fig. 1. At 0°C the R-curve rises relatively steeply because of the high degree of plastic deformation. At -40°C a "pop-in" occurs after a small amount of stable crack growth followed by a region exhibiting extensive stable crack growth. Over the whole transition temperature region the R-curves of the steel 30 CrNiMo 8 are characterized by these sudden unstable crack propagation steps. Even at -100°C the fracture was not completely unstable; the crack had also been arrested, though at a relatively large crack extension.

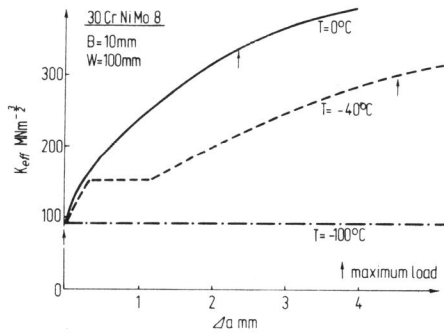


Fig. 10 Effect of temperature on R-curve behaviour $K_{eff}-\Delta a$ for 100 mm wide and 10 mm thick CT-specimens of the steel 30CrNiMo8.

CONCLUSIONS

Three elastic-plastic methods were used to describe the influence of thickness on the R-curves of CT-specimens of the high strength steel 30 CrNiMo 8. The elastic-plastic R-curves in terms of $K_{eff}\sqrt{a}$ and $K_J\sqrt{a}$ were found to agree well up to and beyond the attainment of maximum load. The variation of temperature and specimen thickness showed the expected influence on the R-curves. Higher plastic deformations occurring at lower thicknesses and higher temperatures result in steeper rising R-curves.

REFERENCES

- BS 5762:1979 (1979). Methods for crack opening displacement (COD) testing. British Standards Institution, Gr. 6.
- Clarke, G. A., and co-workers (1978). A procedure for the determination of ductile fracture toughness values using J integral techniques. Westinghouse R and D Center, Scientific Paper 78-1D3-JINTF-P2.
- Hagedorn, K. E., and U. Rüdiger (1977). Ermittlung von Ermüdungsrißlängen in Bruchmechanikproben aus Stahl RSt 37-2 mit dem Potentialsondenverfahren. Arch. Eisenhüttenwes., 48, No. 9.
- Merkle, J. G., and H. T. Corten (1974). A J-integral analysis for the compact specimen, considering axial force as well as bending effects. ASME, Paper No. 74-PVP-33.
- Schmitt, W., and E. Keim (1979). Numerical aspects of elastic-plastic fracture mechanics including 3-D applications. 2nd Advanced Seminar on Fracture Mechanics, Ispra.
- Srawley, J. E., and W. F. Brown Jr. (1965). Fracture toughness testing methods. In ASTM STP 381, Am. Soc. Test. Mats., pp. 133-198.